

Efficient Virtual Screening Using Multiple Protein Conformations Described as Negative Images of the Ligand-Binding Site

Salla I. Virtanen and Olli T. Pentikäinen*

Department of Biological and Environmental Science & Nanoscience Center, P.O. Box 35, FI-40014
University of Jyväskylä, Finland

Received February 1, 2010

The protein structure-based virtual screening is typically accomplished using a molecular docking procedure. However, docking is a fairly slow process that is limited by the available scoring functions that cannot reliably distinguish between active and inactive ligands. In contrast, the ligand-based screening methods that are based on shape similarity identify the active ligands with high accuracy. Here, we show that the usage of negative images of the ligand-binding site, together with shape comparison tools, which are typically used in ligand-based virtual screening, improve the discrimination of active molecules from inactives. In contrast to ligand-based shape comparison, the negative image of the binding site allows identification of compounds whose shape complements the shape of the ligand-binding cavity as closely as possible. Furthermore, the use of several target protein conformations allows the identification of active ligands whose shape is not optimal for crystallized protein conformation. Accordingly, the presented virtual screening method improves the identification of novel lead molecules by concentrating on the optimally shaped molecules for the flexible ligand binding site.

INTRODUCTION

Shape complementarity plays a crucial role in molecular recognition between a small molecule and its protein target. This requirement of complementary shape has been employed in computational chemistry applications such as molecular docking (especially in protein–protein docking)^{1,2} and virtual screening.³ Nevertheless, when evaluating the ligand binding energy, the scoring has not been directed by the shape; instead, the electrostatics are emphasized.

Ligand-based screening methods are efficient in finding active molecules.⁴ In ligand-based virtual screening, the basic idea is to compare: (1) the shape (or shapes) of known ligand(s) with “unknown” ligands or (2) the chemical properties of known molecules described as pharmacophore models. Those methods that are based on ligand similarity comparison can either compare two-dimensional (2D) or three-dimensional (3D) similarity. The 2D similarity methods, such as Daylight fingerprints,⁵ perform surprisingly well in finding active molecules.⁶ However, the resulting high-ranking molecules from the 2D similarity comparison tend to have the same functional groups as the query molecule,^{7,8} and, thus, it is expected that the 3D similarity methods, which concentrate on the volume that the molecule acquires, will find novel lead molecules with a higher degree of scaffold hopping.

The ligand-based approaches that are based on the similarity of the pharmacophoric properties of a known set of molecules are also promising.^{9,10} However, the production of a pharmacophore model requires that several ligands with similar affinities for the target are available for the buildup of the model.⁸ The downside in pharmacophore modeling is that the model does not describe the shape of the ligand-

binding site unless the information from the protein structure is included. The addition of protein structure information complicates the model significantly, and thus the comparisons become computationally demanding.

In the 3D similarity searching software ROCS,¹¹ the pharmacophoric properties, such as hydrogen-bond acceptor or donor, hydrophobe, ring atom, cation or anion, can be implemented to the search. In another similarity searching software (SHAEP),¹² the similarity of the molecules can be calculated with the electrostatic potential taken into account. Although the implementation of chemical properties into the search can be beneficial, the simple use of complementary shape has been used successfully to find new drug candidates. Rush and colleagues, for example, found novel scaffolds to modulate bacterial protein–protein interactions, using the shape of the initial lead molecule from high-throughput screening.³

However, there are cases in which there are no known ligands to the target or the preferred molecule is very different from the established binding molecules. For example, when trying to find ligands that modulate protein–protein interactions, there usually are not any prior molecules that could be used as queries. Unless considering experimental screening campaign, the search for the first binding ligand must employ protein structure-based methods. Molecular docking is a popular method among structure-based approaches and many different software tools have been developed, such as AUTODOCK,¹³ DOCK,¹ GLIDE,¹⁴ GOLD,¹⁵ and FRED.¹⁶ Massive effort has been addressed to the development of docking methods, and, currently, the correct binding mode of the ligands can be predicted fairly efficiently. However, the prediction of the binding affinity has been proven to be more challenging, and, thus, the enrichment may fail in virtual screening.^{4,6,17}

* Author to whom correspondence should be addressed. Tel.: +358-14-260-4186. Fax: +358-14-260-2221. E-mail: olli.t.pentikainen@jyu.fi.

Protein flexibility should also be considered in ligand design. The majority of docking algorithms treat ligands flexibly; however, because of the high computational cost, protein targets are usually considered to be rigid structures. Protein movement has thus far been incorporated into structure-based virtual screening with the use of different rotamers for the amino acid side chains,¹⁸ and the use of multiple protein structures/conformations, that can be either experimentally determined¹⁹ or derived from computational data, such as molecular dynamics (MD) simulations²⁰ or normal-mode analysis.²¹

Here, we describe a protein structure-based method in which a negative image of the ligand binding site is constructed as an atomistic model. This binding-site model can be implemented directly with any ligand shape-based virtual screening software. In the process of the negative image creation, the possible hydrogen bonds that form between a small molecule and the protein are taken into account by allowing the negative image to be closer to the hydrogen-bond-forming atoms in the protein, compared to van der Waals distances. Thus, this model more realistically describes the shape of the optimal ligand molecule. We demonstrate that the negative-image-based method is more successful in virtual screening, compared to structure-based docking software and, in many cases, also produces better results than the ligand-based methods. Furthermore, we show that the usage of multiple protein conformations may increase the success rate in the identification of active ligands. Accordingly, the presented method serves as an excellent starting point for further virtual screening development.

MATERIALS AND METHODS

Proteins and Ligands for Virtual Screening. To validate a virtual screening method, a set of targets and databases for active and decoy molecules are required. The Directory of Useful Decoys (DUD),²² which is the largest freely available database for evaluating docking and virtual screening methods, was employed here. The targets used in our study are listed in Table 1. The protein targets given in ref 22 were downloaded from the Protein Data Bank (PDB).²³

The protein structures (Table 1) were used to create the negative image of the ligand-binding site. Hydrogens were added to the structures with TLEAP (ANTECHAMBER 1.27).²⁴ The bound conformation of the ligand in complex with the crystallized protein was used as a reference in shape comparison. To generate multiple low-energy conformers for each molecule in the datasets, the Schrödinger ConfGen²⁵ routine was employed. ConfGen provides a selection of preset strategies for conformational searching, and, from these, the “fast” option was chosen. The “fast” protocol generates up to five conformers per degree of freedom and eliminates conformers with root mean square deviation (rmsd) values of <1.0 Å. In addition, conformers whose energy was more than 25 kcal/mol higher than the lowest energy conformer were eliminated. A Merck molecular force field (MMFF) was used in the conformational search. A total of 86 decoy molecules were left out of the screening process, because there were no MMFF atom types available for one or more atoms in these molecules. For comparison, the molecule data sets were also tested, as provided within the DUD, to study whether the datasets could be used without further processing for validating ligand-based screening approaches.

Table 1. Targets Used in the Virtual Screening, and Their Corresponding PDB Codes^a

protein ^b	PDB code	number of actives	number of decoys
Nuclear Hormone Receptors			
AR	1xq2 , 2am9, 2ax6, 2oz7, 2pir, 2pnu, 3b5r, 3b65, 3b68	74	2628
ER _{agonist}	1ere, 1gwq, 1l2i , 1lku, 1x7e, 1x7r, 2g44, 2p15, 3erd	67	2352
ER _{antagonist}	3ert	39	1395
GR	1m2z , 1p93, 3bqd, 3cld, 3e7c, 3gn8, 3k23	78	2797
MR	1y9r, 1ya3, 2aa2 , 2aa6, 2aa7, 2aax, 2ab2, 2abi, 2oax	15	534
PPAR _g	1fm9	81	2905
PR	1a28, 1e3k, 1sqn, 1sr7 , 1zuc, 2ovh, 2ovm, 2w8y, 3d90	27	967
RXR _α	1fm9, 1mv9, 1mvc , 1xv9, 1xvp, 2plu, 2plv, 2zxz, 3h0a	20	706
Kinases			
TK	1kim	22	784
VEGFR2	1vr2	74	2640
Folate Enzymes			
DHFR	3dfr	201	7138
Other Enzymes			
COX-2	1cx2	349	12458
HIVRT	1rt1	40	1437
SAHH	1a7a	33	1158

^a Protein structures provided within the Directory of Useful Decoys (DUD) are highlighted in bold type. ^b Abbreviations: AR, androgen receptor; ER, estrogen receptor; GR, glucocorticoid receptor; MR, mineralocorticoid receptor; PPAR_g, peroxisome proliferator activated receptor gamma; PR, progesterone receptor; RXR_α, retinoic X receptor alpha; TK, thymidine kinase; VEGFR2, vascular endothelial growth factor receptor kinase 2; DHFR, dihydrofolate reductase; COX-2, cyclooxygenase 2; HIVRT, human immunodeficiency virus reverse transcriptase; SAHH, S-adenosyl-homocysteine hydrolase.

Atomistic Binding Site Models. In our procedure, the ligand-binding cavity of protein is filled with a cluster of atoms to produce a negative image of the ligand-binding site. This cavity-filling model can also be seen as a ligand-like entity that represents the space available for the actual ligand binding. Two freely available software tools were used for this: (1) PASS (Putative Active Sites with Spheres),²⁶ and (2) VOIDOO/FLOOD;²⁷ of these tools, the latter one was used more routinely, because it allows flexible adjustments of the van der Waal (vdW) parameters (see below).

PASS. For cavity detection, PASS first covers the protein surface with probe spheres, which have radii of 1.5 Å for a protein with hydrogens and 1.8 Å without hydrogens. A filtering step is applied thereafter, in which a “burial count” is calculated for each probe sphere. In the “burial count”, the number of atoms within an 8 Å radius are calculated to determine whether the probe is located within a cavity or on the surface of the protein. A threshold value for the “burial count” is used to determine the burial of the cavities. The threshold is 75 for proteins with hydrogens, and 55 for proteins without hydrogens. Probe spheres with a lower “burial count” than the threshold value are omitted from further calculations, as are the probe spheres that clash with protein atoms. Additional layers of probe spheres are then accreted on the probe spheres located in cavities in an iterative manner until the cavity is filled. PASS identifies all possible cavities into one file, and the correct one was visually selected using a BODIL Modeling Environment.²⁸

The spheres were assigned to be carbon atoms for subsequent shape comparisons.

VOIDOO/FLOOD. VOIDOO/FLOOD was originally developed to aid cavity detection, mainly for crystallographic purposes; however, it has been also widely used to solve the cavity solvation problem in MD simulation studies. In VOIDOO, a 3D grid is first laid on the protein. The cavity detection proceeds by calculating the distance from each grid point to the nearby atoms of the macromolecule. The grid points for which the distance to an atom is less than the sum of the vdW radius of the atom and the probe radius are considered as part of the protein, while where the distance is greater, the grid points are considered as being either inside the cavities or outside the protein. VOIDOO considers only the cavities located within the protein. To detect invaginations in macromolecules that are not totally buried from the surroundings, VOIDOO uses a process called “atomic fattening”. In “atomic fattening”, the vdW radii of every atom are multiplied by a user-specified factor until the “outside world” is excluded. FLOOD is used to fill the cavities detected by VOIDOO with solvent molecules (or other molecules/atoms). FLOOD uses the initial grid points to fill the cavity with as many solvent molecules as possible, considering a user-specified radius of the filling atom, i.e. solvent radius (see Figure 1). For shape comparison, the negative image was assigned to consist of carbon atoms.

Protein Flexibility. A subset of the protein targets was chosen to represent the effect of protein flexibility in the search. The protein flexibility was taken into account by constructing the negative image to either additional protein crystal structures, or by generating new conformations for the proteins with molecular dynamics (MD) simulations. Additional protein crystal structures were downloaded from the PDB database (the PDB codes are listed in Table 1), ligands and water molecules were removed, and the protein structures were superimposed with BODIL.

Molecular Dynamics Simulations. MD simulations were used to create new conformations for the protein crystal structures downloaded from the PDB. For the androgen receptor (AR), a different protein structure than that within the DUD was used (PDB code: 2am9), because of higher resolution (1.9 Å for 1xq2 vs 1.6 Å for 2am9). MD simulations were run with NAMD 2.6,²⁹ and TLEAP was used to (1) create force field parameters for the proteins, (2) add hydrogens, and (3) solvate the protein with a rectangular box of transferable intermolecular potential three-point water molecules (TIP3P), 13 Å in every dimension. To avoid the closure of the ligand-binding cavity during MD simulations, the empty binding site of the protein was filled with water molecules with VOIDOO/FLOOD. Default settings for VOIDOO/FLOOD were used, except the solvent radius in FLOOD was set to 2.1 Å (default 1.4 Å). This was done because it was noticed that, with the default value for the parameter, the ligand-binding site became excessively packed with water molecules and, accordingly, during MD simulation, the binding site enlarged inappropriately (data not shown).

MD simulations were performed as described previously.³⁰ In short, the ligand-free protein structures were first energy-minimized in two steps: the water molecules and amino acid side chains were first minimized with a conjugate gradient algorithm (15 000 steps) with C $^{\alpha}$ -atoms restrained with a harmonic force of 5 kcal mol⁻¹ Å⁻², after which the protein

was minimized without constraints (15 000 steps). The MD simulations were first run at constant volume and temperature for 360 ps (timestep of 2 fs) with C $^{\alpha}$ -atoms restrained as in the minimization step. This was followed by the production simulation of 2.4 ns (timestep of 2 fs) at constant pressure and temperature.

Trajectories. Snapshots at 400 ps intervals were extracted from the MD trajectories with PTRAJ 10 in the ANTECHAMBER 1.27 package.²⁴ To create the multitemplate for shape comparison, negative images were created for the binding sites of the starting crystal structure, energy-minimized structure, and for the snapshots derived from the trajectory.

Shape Comparison. For shape comparison, two different software tools were used: SHAEP¹² and ROCS.¹¹ SHAEP employs a maximal subgraph isomorphism algorithm that superimposes the molecules onto the templates. The superimposition is scored based on the shape-density overlap volume of the molecular shape, which is described by spherical Gaussians. ROCS uses spherical Gaussians to describe the molecular shape, but the superimposed molecules are scored based on Tanimoto-like overlap of molecular volumes. In both softwares, the option that takes into account only the shape of the ligands was used (SHAEP: onlyshape; ROCS: shapeonly). Because both of the used shape comparison tools can accept multiple target structures, the effect of flexibility of proteins was also studied.

Docking. As a reference of structure-based virtual screening, molecular docking with GOLD¹⁵ and GLIDE¹⁴ was applied for a subset of the targets. Since the databases within DUD are prepared for docking with the ZINC³¹ uploading system, molecule datasets were used as provided without further processing. Default settings were used for the docking algorithms, unless otherwise noted.

GOLD. Hydrogens were added to the target proteins with TLEAP. GOLD 4.1 was employed for docking, and the fitness values of the Goldscore were used to evaluate the binding affinity. The binding site was defined by choosing an atom within the cavity, and the active site radius was set to 15 Å. Ring corners and amide bonds were allowed to flip.

GLIDE. For docking with GLIDE 5.5, the protein structures were prepared with the Protein Preparation Wizard in Maestro.³² The protein preparation was done according to the manufacturer's instructions. GLIDE offers three different strategies for docking: high-throughput virtual screening (HTVS), standard precision (SP), and extra precision (XP) options. Considering the size of the databases the HTVS option was used in our studies. It was noticed that GLIDE was not able to dock all the molecules in the datasets. For that reason, the undocked molecules were positioned at the end of the ranking lists by giving arbitrarily bad scoring values. Ligands and decoys were also distributed randomly, so that the subsequent analyses of the virtual screening efficiency would correspond random selection of these molecules.

Metrics. The efficiency by which the method is able to enrich the active ligands from the database was depicted by calculating receiver-operating characteristics (ROC) curves. The area under the curve (AUC) equals the probability of ranking randomly selected active molecule higher than randomly selected inactive molecule.³³ A diagonal line with AUC = 0.5 describes a situation where random picking of

the molecules is evenly as good as the tested method, whereas for an ideal screening method, AUC = 1.

Figures. Figures 1 and 3 were prepared by using BODIL²⁸ (surfaces), MOLSCRIPT³⁴ (atom and secondary structure information), and RASTER3D³⁵ (rendering).

RESULTS

The objective of this work was to produce a simple, fast, and efficient method that would employ a protein structure in virtual high-throughput screening (vHTS). For this purpose, negative image models for the ligand-binding sites of selected proteins were built. To allow easier development of the method in the future, i.e., incorporation of additional information to the model, shape comparison software tools that can use atom information were chosen. The creation of such a negative image that could mimic a small binding molecule was performed using freely available cavity detection software.

Optimization of VOIDOO/FLOOD Parameters. The default parameters in VOIDOO for cavity detection and filling were modified to get binding-site filling atoms into reasonable distances from the protein. For example, hydrogen bonds can exist, if the atom radii distances between non-hydrogen atoms are as low as 2.6 Å; however, vdW interactions most likely dominate from 3.6 Å upward. Such distances were obtained using a radius of 1.25 Å for the probe to define the ligand-binding cavity (default = 1.4 Å), and the radius for carbon atoms was increased from 1.85 Å to 2.25 Å, leading to a distance of 3.50 Å between the protein and the negative image. Radii for oxygen and nitrogen atoms was reduced to 1.2 Å from 1.6 Å and 1.75 Å, respectively, leading to distances of 2.45 Å. The use of grid-based methods to fill the cavity very seldom produces the minimum values for the hydrogen-bonding or vdW distances. This is compensated by allowing the distances to be shorter during the cavity detection: 2.45 Å for hydrogen bonds, instead of 2.6 Å, and 3.5 Å for vdW interactions, instead of 3.6 Å. A multitude of combinations with different atom radii were used in the optimization of software settings. The vdW growth factor was set to 1.2, to enable the discovery of cavities that were not entirely buried from the surrounding solvent.

Figure 1A shows the ligand-binding site of a glucocorticoid receptor (GR) detected by VOIDOO. When default solvent radius parameters for FLOOD were used (1.4 Å), the atoms were too far apart from each other to mimic a real molecule (see Figure 1B), resulting in a model that does not represent the shape of the cavity well enough. Thus, different values for solvent radius in FLOOD, ranging from 0.35 Å to 1.5 Å, were tested to determine the optimal value (Figure 2). Optimization of the solvent radius was performed with cyclooxygenase 2 (COX-2), estrogen receptor (ER) agonist, mineralocorticoid receptor (MR), and GR. With the solvent radii at <0.65 Å, the relative computation time increased notably (see dotted line in Figure 2), because the number of atoms in the model becomes high. The obtained AUC values were generally higher with the solvent radius <1.0 Å. A solvent radius of 0.7 Å was chosen, because it provided both efficient computation and high AUC value. In addition, the model consists of atoms with interatomic distances of 1.4 Å, thus representing an average of single and double bonds between two carbon atoms (see Figure 1C), and, accordingly,

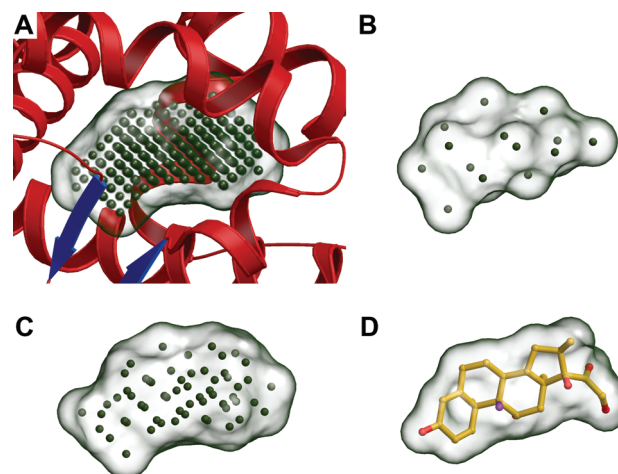


Figure 1. Atomistic model of the ligand binding site of glucocorticoid receptor. In panel (A), the grid-based positions that were identified with VOIDOO are shown. In panels (B) and (C), the VOIDOO-based cavity was filled with solvent molecules, whose radii are 1.4 Å and 0.7 Å, respectively. For comparison, panel (D) shows the ligand from the crystal structure of glucocorticoid receptor (PDB code: 1m2z). The surfaces in each panel show the solvent-accessible surface of the given atoms/points. The FLOOD model points were considered as carbon atoms in the surface calculation.

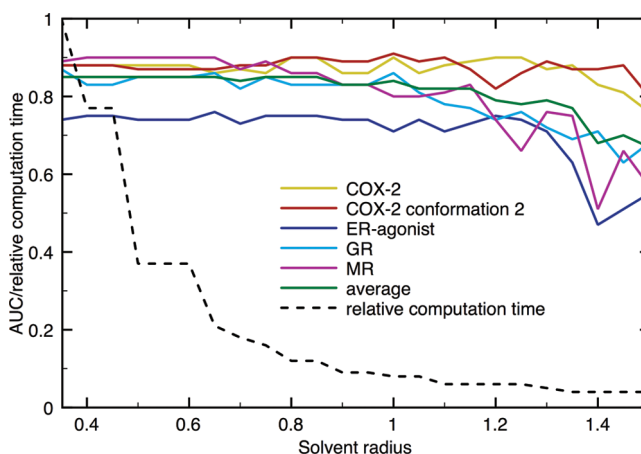


Figure 2. Effect of solvent radii in FLOOD to the AUC values (solid lines) and the relative computation time for the comparison (dotted line).

the model resembles a real ligand molecule (see Figure 1D) and the binding cavity is filled efficiently.

In grid-based methods, the orientation of the protein in 3D affects how the grid points are located on the protein. In the original paper, Kleywegt et al.²⁷ suggested that VOIDOO should be run for multiple randomly rotated proteins to avoid inaccuracies in the volume calculations. For that reason, the negative image was constructed for a randomly rotated COX-2 structure, to test whether the positioning of the grid affects the resulting model (see COX-2 conformation 2 in Figure 2). If two different orientations of the protein were used for the negative-image generation, the AUC values differed only slightly with the solvent radius being <0.85 Å, but the differences increased when the radius was set at >0.90 Å. This makes sense, because the use of a low solvent radius enables closer packing of solvent molecules and therefore describes the shape of the binding site better, whereas if a higher solvent radius is used, the atoms in the negative image may not be optimally located to resemble

Table 2. ROC AUC Values for Selected Targets^a

target	SHAEP									
	Docking		SHAEP				ROCS		SHAEP	
	GLIDE	GOLD	DUD original ^b		DUD mmff ^c		ligand	model	multi X-ray	MD
AR	0.73 ± 0.03	0.26 ± 0.03	0.81 ± 0.03	0.87 ± 0.03	0.80 ± 0.03	0.84 ± 0.03	0.70 ± 0.04	0.83 ± 0.02	0.87 ± 0.03 (9)	0.80 ± 0.03 (8)
ER-ago	0.81 ± 0.03	0.37 ± 0.03	0.73 ± 0.04	0.82 ± 0.03	0.76 ± 0.03	0.79 ± 0.03	0.76 ± 0.04	0.75 ± 0.04	0.84 ± 0.03 (9)	0.82 ± 0.03 (8)
ER-anta	0.68 ± 0.05	0.60 ± 0.04	0.73 ± 0.05	0.64 ± 0.05	0.81 ± 0.04	0.75 ± 0.05	0.84 ± 0.03	0.66 ± 0.06	nd	nd
GR	nd	nd	0.74 ± 0.03	0.91 ± 0.02	0.61 ± 0.03	0.85 ± 0.03	0.52 ± 0.04	0.80 ± 0.03	0.81 ± 0.03 (7)	0.76 ± 0.03 (9)
MR	0.73 ± 0.05	0.68 ± 0.05	0.79 ± 0.07	0.90 ± 0.05	0.79 ± 0.07	0.91 ± 0.05	0.83 ± 0.08	0.91 ± 0.02	0.91 ± 0.05 (9)	0.86 ± 0.06 (9)
PPAR _g	nd	nd	0.70 ± 0.03	0.79 ± 0.03	0.72 ± 0.03	0.67 ± 0.03	0.75 ± 0.03	0.70 ± 0.03	nd	nd
PR	0.54 ± 0.06	0.37 ± 0.06	0.78 ± 0.05	0.67 ± 0.06	0.50 ± 0.06	0.50 ± 0.06	0.32 ± 0.06	0.42 ± 0.08	0.79 ± 0.05 (9)	0.87 ± 0.04 (9)
PR (1a28)	nd	nd	0.70 ± 0.06	0.80 ± 0.05	0.67 ± 0.06	0.67 ± 0.06	0.64 ± 0.07	0.49 ± 0.07	nd	nd
RXR _α	0.85 ± 0.04	0.60 ± 0.04	0.79 ± 0.06	0.93 ± 0.04	0.92 ± 0.04	0.99 ± 0.01	0.92 ± 0.04	0.93 ± 0.02	0.97 ± 0.03 (9)	0.94 ± 0.04 (7)
COX-2	nd	nd	0.90 ± 0.01	0.91 ± 0.01	0.87 ± 0.01	0.85 ± 0.01	0.95 ± 0.01	0.89 ± 0.01	nd	nd

^a The best AUC values are highlighted in bold type, and the lowest values are shown in italic font. Numbers given in parentheses correspond to the number of protein structures or conformations used. nd = not determined. ^b DUD datasets used without processing. ^c Multiple low-energy conformations generated for each molecule with MMFF force field.

the desired molecule correctly. In subsequent studies, only one protein orientation was used that was obtained from the original crystal structure, because the grid positioning had only a minor effect on the results with low solvent radii. In addition, the objective in this study was to describe the shapes of the binding sites in atomistic terms, not to measure the exact volumes of the cavities.

Single Targets. Virtual screening was performed to the set of nuclear hormone receptors and COX-2 with the negative image created with VOIDOO (see “model” columns in Table 2), and the ligand from the crystal structure was used as a reference (see “ligand” columns in Table 2). Shape comparisons were made with both SHAEP and ROCS. For comparison, molecular docking was performed with GLIDE and GOLD for selected targets (see Table 2).

The test runs were also made with the unmodified DUD sets, which contain only one conformer for the molecule. The results show similar AUC values for both the unmodified set and the set of conformers generated with ConfGen (see Table 2). This implies that a single low-energy conformation for each molecule also could be used in virtual screening.

The docking results show that GLIDE produces higher enrichment than GOLD. Particularly, for AR and ER_{agonist}, the AUC values with GOLD are extremely low, compared to GLIDE, which could achieve comparatively high AUC values for those targets. In DUD, some ligand collections are very similar to each other, which is notable especially with RXR. This is reflected in the AUC values that show generally high enrichment rates with different screening methods. Keeping this in mind, the poor success of the docking–scoring combination in the case of GOLD is even more surprising, because the crystal structure where ligands and decoy molecules were docked had originally bound one of these ligands.

For PR, the AUC value is near or below random with all the tested screening methods. Visual inspection of the ligands reveals that the set contains molecules with various different sizes and shapes. For this reason, one ligand or negative image of the ligand binding site does not represent the wide variety of the ligands well. This suggests that the use of different protein structures for negative-image creation could increase the enrichment of actives. Accordingly, another PDB structure for PR with bound progesterone was used (PDB code: 1a28) for comparison. When this other protein structure was used, the AUC value increased from 0.50 up to 0.67

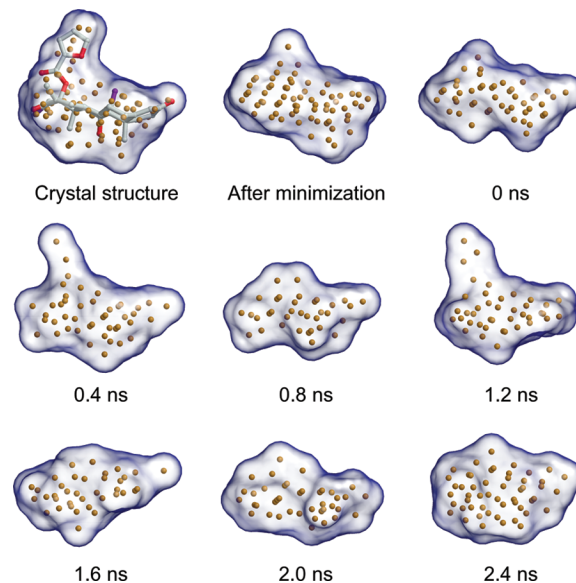


Figure 3. Atomistic models for the crystal structure of progesterone receptor (PDB code: 1sr7) and derived MD snapshots. The ligand from the crystal structure is shown for comparison in the first figure.

when SHAEP was used in the shape comparison. Although the result is still quite poor, the improvement is clear, and it demonstrates well the importance of choosing the right template, whether it is an actual ligand molecule or a model based on the shape of the ligand-binding site.

Multitargets. To include protein flexibility into the search, additional experimentally resolved protein crystal structures and new conformations created with MD simulations were used in the generation of the negative image for a subset of the targets (see Table 1). Generally, the use of multiple crystal structures shows slightly better performance over the use of conformations generated through MD simulations. However, PR is an exception for this, because the use of conformations derived from MD snapshots enhances greatly the virtual screening success. The resulting negative images of the MD snapshots for PR reveal that the amino acids surrounding the ligand-binding pocket are highly flexible, and, thus, a multitude of alternative shapes that the ligand can use in binding exist (see Figure 3).

PASS Results. PASS was also tested for the creation of the negative image. PASS is a fast method for cavity detection; the downside, however, is that the parameters are

Table 3. AUC Values When PASS Was Employed in Cavity Detection and SHAEP Was Used in the Similarity Comparison

target	model with PASS	ligand
DHFR	0.63 ± 0.02	0.53 ± 0.02
HIVRT	0.69 ± 0.05	0.70 ± 0.05
SAHH	0.76 ± 0.05	0.86 ± 0.04
TK	0.63 ± 0.06	0.83 ± 0.05
VEGFR2	0.58 ± 0.04	0.44 ± 0.03
AR	0.80 ± 0.03	0.80 ± 0.03
ER _{agonist}	0.76 ± 0.03	0.76 ± 0.03
ER _{antagonist}	0.76 ± 0.05	0.81 ± 0.04
GR	0.80 ± 0.03	0.61 ± 0.03
MR	0.92 ± 0.05	0.79 ± 0.07
PPAR _g	cavity not found	0.72 ± 0.03
PR	0.54 ± 0.06	0.50 ± 0.06
RXR _α	0.83 ± 0.06	0.92 ± 0.04
COX-2	cavity not found	0.87 ± 0.01

not adjustable. The separation of points cannot be varied and the pockets are filled using standard vdW distances, and, accordingly, the positions for hydrogen-bonding interactions are not filled. Table 3 shows the results when PASS was used to create a negative image of the binding site for the nuclear hormone receptors, dihydrofolate reductase (DHFR), human immunodeficiency virus reverse transcriptase (HIVRT), *S*-adenosyl-homocysteine hydrolase (SAHH), thymidine kinase (TK), and vascular endothelial growth factor receptor kinase 2 (VEGFR2). The results show that, despite its limitations, PASS was also able to create negative images of the ligand binding site that produced reasonable AUC values. The advantage of PASS over VOIDOO/FLOOD is that it also can identify cavities at the surface of the protein, thus significantly widening the assortment of possible targets. For example, PASS managed to identify easily the ligand-binding sites of DHFR, HIVRT, SAHH, TK, and VEGFR2.

DISCUSSION

Here, we have described a method that uses the shape of the ligand-binding pocket to identify active ligands from inactive molecules. The comparison of the small molecules against the ligand-binding site model was performed using two shape comparison software tools that are typically used in ligand-based drug discovery: ROCS and SHAEP. Because both of the shape comparison tools used can accept multiple target structures, the flexibility of proteins was also included into shape comparisons. Protein flexibility was added using multiple crystal structures or consecutive snapshots from MD simulations. For most of the targets, the use of multiple crystal structures provided a slightly higher enrichment of active molecules than conformations from MD simulations, whereas for PR, the situation was the opposite. This indicates that conformations derived with MD simulations can provide a means on how to discover active molecules with different shapes and, also, in a wider context, pinpoints the crucial importance of protein flexibility in ligand discovery. In the present study, we show that the developed method gives better results than the scoring functions implemented into docking software tools and yields comparable efficiency to that of ligand-based screening.

The validation of the presented method was done using the DUD datasets for ligands and decoy molecules. Although the DUD database has its limitations—for example, the ligand

sets are not diverse in all cases—it has been widely used in many recent validation studies for both structure- and ligand-based virtual screening approaches.^{10,12,38} Accordingly, it was logical to use the DUD dataset in this study as well. The diversity problem reflects most directly into the usage of a single ligand or protein model, because the result is strongly biased by the similarity of the ligands, and thus, the enrichment can be unreasonably high for the sets that have highly similar ligands. Similarly, when the ligand set is highly diverse, as in the case of PR, a single molecule or protein model cannot separate active ligands from inactive molecules. Immediately when multiple PR conformations were used as targets, the ligands were identified from inactive molecules with higher accuracy. Since the DUD was developed for validating docking methods, it has been argued that the results are biased toward ligand-based methods when different screening approaches are compared. Thus, the possible bias in the results must be taken into account when comparing structure- and ligand-based methods with this dataset.

Although the current shape-based protocol can rapidly and quite efficiently separate active ligands from inactive molecules, there are obvious possibilities for the improvement of the protocol:

(1) Each model point can contain additional information such as electrostatics in the form of partial charges or pharmacophoric properties.

(2) The top-ranked molecules could be re-evaluated with secondary screening protocol, such as the Molecular Mechanics-Poisson–Boltzmann Surface Area (MM-PBSA) method.³⁶

(3) Water molecules that may participate into ligand binding, or that can be replaced by the ligand, can be included into the model. Accordingly, ligands that are not able to fill the entire cavity would not be discriminated.

(4) When both protein structure information and ligand information are available, these data can be combined into one model.

During the preparation of this manuscript, studies describing related methods were published by Ebalunode et al.³⁷ and Lee et al.³⁸ In the article by Ebalunode and colleagues,³⁷ the negative image of the ligand-binding site was constructed with a software tool distributed by OpenEye, which employs alpha-shapes to define the ligand-binding cavity. The similarity between the negative image and the molecules was then compared with ROCS. They included pharmacophoric features into the search and used ROCS-color to evaluate the similarity in combination with shape, and this combined method was able to discriminate the actives from decoy molecules better than the shape comparison or FRED ShapeGauss alone. Lee et al.³⁸ used a grid-based approach to make a negative image of the binding site of the protein, which was subsequently used with ROCS to screen active ligands. They also extracted pharmacophoric features from the protein structure, and the method was able to outperform the same docking software tools as those used in our study (GLIDE and GOLD). However, in the methods reported by Ebalunode et al.³⁷ and Lee et al.,³⁸ the negative image was created directly, according to the binding site shape, whereas in our approach, the negative image is allowed to go closer to the protein in places where hydrogen bonds may occur, and thus the model more realistically resembles an active molecule. In fact, we got high enrichment of active molecules

using only the shape of the negative image as a search criterion. However, as mentioned previously, the incorporation of chemical information to the model in the form of electrostatics or pharmacophoric properties could further improve the efficiency.

CONCLUSIONS

So far, the protein-structure-based virtual screening methods have been heavily concentrated on molecular docking. However, because the main idea in virtual screening is to rapidly screen large molecule databases (e.g., all commercially available molecules or even larger virtual combinatorial chemistry libraries), the scoring of docking results has not been able to reliably discriminate inactive ligands from actives. The method developed here employs a simple shape comparison method previously used in ligand-based ligand discovery. Although in ligand-based discovery, the molecules are compared to known ligand(s), here, we suggest an alternative method where a negative image of the target protein's ligand binding site is created. The negative image consists of simple spheres that can be considered as atoms of an optimally shaped ligand. Protein dynamics can be included to the ligand discovery via the use of multiple protein conformations derived from either experimental data or computational methods. In all, the developed method shows excellent enrichment in ligand identification from a set of molecules, and it can be valuable tool in future drug discovery studies.

ACKNOWLEDGMENT

This study was financially supported by the Sigrid Jusélius Foundation (OTP) and Emil Aaltonen Foundation (SIV). CSC, the Finnish IT Center for Science (Espoo, Finland), is acknowledged for the access to the generous computational resources (through Project Nos. jyy2516 and gc2571). The authors wish to thank M.Sc. Pekka Postila for valuable discussions during the manuscript preparation.

REFERENCES AND NOTES

- Shoichet, B. K.; Bodian, D. L.; Kuntz, I. D. Molecular docking using shape descriptors. *J. Comput. Chem.* **1992**, *13*, 380–397.
- Gabb, H. A.; Jackson, R. M.; Sternberg, M. J. Modelling protein docking using shape complementarity, electrostatics and biochemical information. *J. Mol. Biol.* **1997**, *272*, 106–120.
- Rush, T. S., III; Grant, J. A.; Mosyak, L.; Nicholls, A. A shape-based 3-d scaffold hopping method and its application to a bacterial protein-protein interaction. *J. Med. Chem.* **2005**, *48*, 1489–1495.
- Hawkins, P. C. D.; Skillman, A. G.; Nicholls, A. Comparison of shape-matching and docking as virtual screening tools. *J. Med. Chem.* **2007**, *50*, 74–82.
- Daylight, Version 4.9; Daylight Chemical Information Systems, Inc.: Aliso Viejo, CA, 2008.
- McGaughey, G. B.; Sheridan, R. P.; Bayly, C. I.; Culberson, J. C.; Kreatsoulas, C.; Lindsley, S.; Maiorov, V.; Truchon, J.; Cornell, W. D. Comparison of topological, shape, and docking methods in virtual screening. *J. Chem. Inf. Model.* **2007**, *47*, 1504–1519.
- Thimm, M.; Goede, A.; Hougardy, S.; Preissner, R. Comparison of 2D similarity and 3D superposition. Application to searching a conformational drug database. *J. Chem. Inf. Comput. Sci.* **2004**, *44*, 1816–1822.
- Leach, A. R.; Gillet, V. J.; Lewis, R. A.; Taylor, R. Three-dimensional pharmacophore methods in drug discovery. *J. Med. Chem.* **2010**, *53*, 539–558.
- Chen, Z.; Li, H.; Zhang, Q.; Bao, X.; Yu, K.; Luo, X.; Zhu, W.; Jiang, H. Pharmacophore-based virtual screening versus docking-based virtual screening: A benchmark comparison against eight targets. *Acta Pharmacol. Sin.* **2009**, *30*, 1694–1708.
- von Korff, M.; Freyss, J.; Sander, T. Comparison of ligand- and structure-based virtual screening on the DUD data set. *J. Chem. Inf. Model.* **2009**, *49*, 209–231.
- ROCS, Version 2.4.2; OpenEye Scientific Software: Santa Fe, NM, 2009.
- Vainio, M. J.; Puranen, J. S.; Johnson, M. S. Shaep: molecular overlay based on shape and electrostatic potential. *J. Chem. Inf. Model.* **2009**, *49*, 492–502.
- Morris, G. M.; Goodsell, D. S.; Huey, R.; Olson, A. J. Distributed automated docking of flexible ligands to proteins: Parallel applications of autodock 2.4. *J. Comput.-Aided Mol. Des.* **1996**, *10*, 293–304.
- Glide, Version 5.5; Schrödinger, LLC: New York, 2009.
- Verdonk, M. L.; Cole, J. C.; Hartshorn, M. J.; Murray, C. W.; Taylor, R. D. Improved protein-ligand docking using gold. *Proteins* **2003**, *52*, 609–623.
- McGann, M. R.; Almond, H. R.; Nicholls, A.; Grant, J. A.; Brown, F. K. Gaussian docking functions. *Biopolymers* **2003**, *68*, 76–90.
- Venhorst, J.; Núñez, S.; Terpstra, J. W.; Kruse, C. G. Assessment of scaffold hopping efficiency by use of molecular interaction fingerprints. *J. Med. Chem.* **2008**, *51*, 3222–3229.
- Leach, A. R. Ligand docking to proteins with discrete side-chain flexibility. *J. Mol. Biol.* **1994**, *235*, 345–356.
- Knegtel, R. M.; Kuntz, I. D.; Oshiro, C. M. Molecular docking to ensembles of protein structures. *J. Mol. Biol.* **1997**, *266*, 424–440.
- Mangoni, M.; Roccatano, D.; Di Nola, A. Docking of flexible ligands to flexible receptors in solution by molecular dynamics simulation. *Proteins* **1999**, *35*, 153–162.
- Cavasotto, C. N.; Kovacs, J. A.; Abagyan, R. A. Representing receptor flexibility in ligand docking through relevant normal modes. *J. Am. Chem. Soc.* **2005**, *127*, 9632–9640.
- Huang, N.; Shoichet, B. K.; Irwin, J. J. Benchmarking sets for molecular docking. *J. Med. Chem.* **2006**, *49*, 6789–6801.
- Berman, H. M.; Westbrook, J.; Feng, Z.; Gilliland, G.; Bhat, T. N.; Weissig, H.; Shindyalov, I. N.; Bourne, P. E. The Protein Data Bank. *Nucleic Acids Res.* **2000**, *28*, 235–242.
- Wang, J.; Wang, W.; Kollman, P. A.; Case, D. A. Automatic atom type and bond type perception in molecular mechanical calculations. *J. Mol. Graphics Modell.* **2006**, *25*, 247–260.
- ConfGen, Version 2.1; Schrödinger, LLC: New York, 2009.
- Brady, G. P. J.; Stouten, P. F. Fast prediction and visualization of protein binding pockets with pass. *J. Comput.-Aided Mol. Des.* **2000**, *14*, 383–401.
- Kleywegt, G. J.; Jones, T. A. Detection, delineation, measurement and display of cavities in macromolecular structures. *Acta Crystallogr., Sect. D: Biol. Crystallogr.* **1994**, *50*, 178–185.
- Lehtonen, J. V.; Stül, D.; Rantanen, V.; Ekholm, J.; Björklund, D.; Ifitkhar, Z.; Huhtala, M.; Repo, S.; Jussila, A.; Jaakkola, J.; Pentikäinen, O.; Nyrönen, T.; Salminen, T.; Gyllenberg, M.; Johnson, M. S. Bodil: a molecular modeling environment for structure-function analysis and drug design. *J. Comput.-Aided Mol. Des.* **2004**, *18*, 401–419.
- Phillips, J. C.; Braun, R.; Wang, W.; Gumbart, J.; Tajkhorshid, E.; Villa, E.; Chipot, C.; Skeel, R. D.; Kalé, L.; Schulten, K. Scalable molecular dynamics with namd. *J. Comput. Chem.* **2005**, *26*, 1781–1802.
- Postila, P. A.; Swanson, G. T.; Pentikäinen, O. T. Exploring kainate receptor pharmacology using molecular dynamics simulations. *Neuropharmacology* **2010**, *58*, 515–527.
- Irwin, J. J.; Shoichet, B. K. ZINC—A free database of commercially available compounds for virtual screening. *J. Chem. Inf. Model.* **2005**, *45*, 177–182.
- Maestro, Version 9.0; Schrödinger, LLC: New York, 2009.
- Hanley, J. A.; McNeil, B. J. The meaning and use of the area under a receiver operating characteristic (ROC) curve. *Radiology* **1982**, *143*, 29–36.
- Kraulis, P. J. Molscript: A program to produce both detailed and schematic plots of protein structures. *J. Appl. Crystallogr.* **1991**, *24*, 946–950.
- Merritt, E. A.; Bacon, D. J. Raster3d: Photorealistic molecular graphics. *Methods Enzymol.* **1997**, *277*, 505–524.
- Kollman, P. A.; Massova, I.; Reyes, C.; Kuhn, B.; Huo, S.; Chong, L.; Lee, M.; Lee, T.; Duan, Y.; Wang, W.; Donini, O.; Cieplak, P.; Srinivasan, J.; Case, D. A.; Cheatham, T. E. Calculating structures and free energies of complex molecules combining molecular mechanics and continuum models. *Acc. Chem. Res.* **2000**, *33*, 889–897.
- Ebalunode, J. O.; Ouyang, Z.; Liang, J.; Zheng, W. Novel approach to structure-based pharmacophore search using computational geometry and shape matching techniques. *J. Chem. Inf. Model.* **2008**, *48*, 889–901.
- Lee, H. S.; Lee, C. S.; Kim, J. S.; Kim, D. H.; Choe, H. Improving virtual screening performance against conformational variations of receptors by shape matching with ligand binding pocket. *J. Chem. Inf. Model.* **2009**, *49*, 2419–2428.